Journal of Hazardous Materials 194 (2011) 243–249

Contents lists available at ScienceDirect

Journal of Hazardous Materials

journal homepage: www.elsevier.com/locate/jhazmat

Fabrication of WO_3/Cu_2O composite films and their photocatalytic activity

Shouqiang Wei*, Yuyan Ma, Yuye Chen, Long Liu, Ying Liu, Zhongcai Shao

School of Environmental and Chemical Engineering, Shenyang Ligong University, Nanping Middle Road 6 #, Shenyang 110159, Liaoning Province, PR China

ARTICLE INFO

Article history:
Received 21 December 2010
Received in revised form 11 July 2011
Accepted 26 July 2011
Available online 5 August 2011

Keywords:
Tungsten trioxide
Cuprous oxide
Electrodeposition
Heterojunction
Photocatalysis
Orange II
Hexavalent chromium

ABSTRACT

WO_3/n-Cu_2O and WO_3/p-Cu_2O composite films have been fabricated on titanium (Ti) substrates with a consecutive cathodic electrodeposition route. Those resulting films were characterized with X-ray diffraction (XRD) and scanning electron microscopy (SEM). Their photocatalytic activity under simulated natural light illumination was evaluated using Orange II (mainly) and Cr(VI) as model pollutants. The results indicate that WO_3/p-Cu_2O exhibits higher photocatalytic activity compared to both WO_3 and p-Cu_2O alone, while the photocatalytic activity of WO_3/n-Cu_2O is higher than WO_3, but lower than n-Cu_2O. Even in the absence of other reducing agents (hole scavengers), WO_3/p-Cu_2O also show certain photocatalytic activity towards reduction of Cr(VI). The photocatalytic activity of WO_3/p-Cu_2O is closely related to the deposition amount of p-Cu_2O. Additionally, WO_3/p-Cu_2O composite film also possesses a relatively high stability during the reactions. The difference in photocatalytic activity between the two types of composite films is interpreted in terms of different mechanisms for transfer of charge carriers photogenerated within the heterojunctions.

1. Introduction

Photocatalytic treatment of organic or inorganic pollutants from water and air using semiconductors as photocatalysts has been a promising process among advanced oxidation technologies [1,2]. Among the photocatalysts, semiconductor TiO_2 has been wildly used for photocatalytic degradation of organic pollutants and photocatalytic reduction inorganic pollutants due to its strong photocatalytic activity, chemical inertness and exceptional chemical and photoelectrochemical stability in aqueous media [3,4]. Unfortunately, its large band-gap (3.2 eV or 380 nm in wavelength units) does not allow the utilization of visible light. WO_3, a n-type semiconductor, has a broad range of band-gap values (2.6–3.3 eV), which means that the photoresponse of WO_3 extends much more into the visible wavelength range in comparison with TiO_2. Furthermore, WO_3 shares many of the same attributes with TiO_2 mentioned above [5]. However, it should be emphasized that the photocatalytic characteristics of WO_3 have not been studied as extensively as those of TiO_2 [6]. The previous researches have shown that WO_3 itself is not effective as photocatalyst [7–9]. One possible reason may be that the fast recombination rate for electron-hole pairs photogenerated in WO_3 reduces its photocatalytic efficiency [7,10]. An effective approach to increase the efficiency of charge separation involves coupling of two or more semiconductors with appropriate energy levels [10]. Many studies have indicated that combination of WO_3 with another semiconductor having broader-band-gap, such as TiO_2 [11,12] and ZnO [9] results in a better separation of the charge carriers in comparison with the single semiconductor materials. Most recently, the combination of WO_3 with semiconductors having lower-band-gap has attracted attention, including $CaFe_2O_4$ (1.85 eV) [13], Fe_2O_3 (1.97 eV) [14], $BiVO_4$ (2.4 eV) [15], $CuBi_2O_4$ (1.5 eV) [16] and CdS (2.25 eV) [10]. Hu et al. [17] reported that p-type Cu_2O powders (1.9–2.0 eV) obtained by scraping the electrodeposited films off the substrate exhibited photocatalytic activity in H_2 generation in the presence of WO_3 powders. However, as to wastewater treatment, film-type photocatalysts present interesting characteristics of easy separation from the treated wastewater after reaction and avoiding the aggregation of particles occurring in the case of suspended powder-type photocatalysts.

Semiconductors are usually prepared by high temperature solidification methods from the elements in bulk form, or vapor phase and vacuum methods in the form of thin films [18]. Because electrodeposition of semiconducting materials presents several advantages in comparison with theses methods: low capital cost, possibility of large-scale deposition, low temperature processing and direct control of film thickness, preparation of semiconductors with electrodeposition methods has received much attention recently [19]. Many oxides and sulfides, such as TiO_2, ZnO, WO_3 and CdS have been prepared with electrodeposition [5,7,19,20]. Cu_2O films can also be electrochemically deposited on conducting substrates, and it was found that Cu_2O deposited at solution pH above 9.0 in an aqueous solution containing 0.4 M copper sulfate and 3 M lactic acid was p-type, while Cu_2O deposited at solution pH

* Corresponding author. Tel.: +86 24 24681936; fax: +86 24 86259041.
E-mail address: weisq1961@126.com (S. Wei).

0304-3894/$ – see front matter © 2011 Elsevier B.V. All rights reserved.
doi:10.1016/j.jhazmat.2011.07.096

below 8.0 or in a different electrolyte solution at low solution pH was n-type [21,22]. In the past several years, composite semiconductors such as WO_3/TiO_2 [7], p-Cu_2O/n-Cu_2O [21], CdS/ZnO [23] and CuO/ZnO [24] have been fabricated with consecutive cathodic electrodeposition or cathodic co-electrodeposition. To the best of our knowledge, there is no report on fabrication of WO_3/p-Cu_2O and WO_3/n-Cu_2O composite films with electrodeposition and evaluation of their photocatalytic activity to degradation of organic pollutants.

In the present work, WO_3/p-Cu_2O and WO_3/n-Cu_2O composite films have been successfully prepared with consecutive cathodic electrodeposition on titanium (Ti) substrates. The obtained composite films were characterized with X-ray diffraction (XRD) and scanning electron microscopy (SEM). Orange II (mainly) was used as model organic pollutant to evaluate the photocatalytic activity of both WO_3/p-Cu_2O and WO_3/n-Cu_2O composite films under simulated natural light illumination. The mechanisms for the charge separation between the heterojunctions are also discussed.

2. Experimental

2.1. Materials

All chemicals were of analytic reagent grade and used as received. Except Potassium dichromate (from Tianjin Damao Chemical Reagent Factory, China), the other reagents were purchased from Sinopharm Chemical Reagent Co. Ltd, China. All solutions were prepared with distilled water.

2.2. Preparation of films

All the elctrodeposition experiments were carried out at constant current density in an ordinary cell using a Pt coil as the counter electrode (anode). Before use, Ti plates used as substrates ($2 \times 3\,cm^2$) were degreased with acetone and etched in a 1–1 HCl/H_2O mixture for 60 s [7]. Cathodic electrodeposition of WO_3 onto Ti substrates (efficient area: $4\,cm^2$) was performed from a bath of pH 1.4 containing 0.013 mol L^{-1} Na_2WO_4, 0.03 mol L^{-1} H_2O_2 and 0.05 mol L^{-1} HNO_3 at room temperature ($25 \pm 1\,^{\circ}C$) for 30 min. The cathodic current density was fixed at 5 mA cm^{-2}. The deposition amount of WO_3 was 9 mg cm^{-2}. The electrodeposition process involves the reduction of the dimeric peroxytungstate species to WO_3 and molecular oxygen according to the following reaction [25]:

$$W_2O_{11}{}^{2-} + (2+x)H^+ + xe^- \rightarrow 2WO_3 + (2+x)/2H_2O + (8-x)/4O_2 \quad (1)$$

WO_3/n-Cu_2O and WO_3/p-Cu_2O composite films were fabricated by subsequent deposition of n-Cu_2O and p-Cu_2O onto the resulting WO_3 films from different electrolyte solutions at cathodic current densities of 0.5 mA cm^{-2} and 1 mA cm^{-2}, respectively. For n-Cu_2O, the electrolyte solution (pH = 5.7) contained 0.01 mol L^{-1} copper acetate and 0.1 mol L^{-1} sodium acetate [21], while the solution for p-Cu_2O (pH = 11) contained 0.4 mol L^{-1} copper sulfate and 3 mol L^{-1} lactic acid [17]. The solution temperature was fixed at 55 °C and 30 °C, respectively. The deposition of n-Cu_2O proceeded for 10 min, and its deposition amount was 0.1 mg cm^{-2}. When the deposition time was 2 min, 5 min, 10 min, 15 min, and 20 min, the corresponding deposition amount of p-Cu_2O was 0.04 mg cm^{-2}, 0.1 mg cm^{-2}, 0.2 mg cm^{-2}, 0.3 mg cm^{-2} and 0.4 mg cm^{-2}, respectively. The electrodeposition reactions for n-Cu_2O and p-Cu_2O may be expressed as follows [26,27]:

$$2Cu^{2+} + H_2O + 2e^- \rightarrow Cu_2O + 2H^+ \quad (2)$$

$$2Cu^{2+} + 2OH^- + 2e^- \rightarrow Cu_2O + H_2O \quad (3)$$

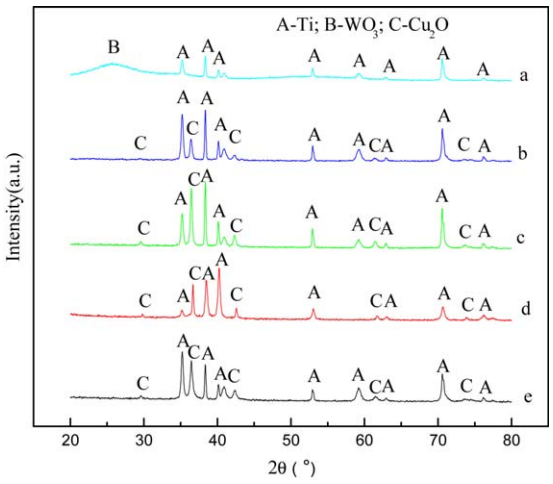

Fig. 1. XRD patterns of WO_3 (a), n-Cu_2O (b), p-Cu_2O (c), WO_3/n-Cu_2O (d) and WO_3/p-Cu_2O (e) films.

Single n-Cu_2O and p-Cu_2O films were obtained by direct deposition of n-Cu_2O or p-Cu_2O onto Ti substrates under the same conditions as mentioned above, respectively. The deposition amount of p-Cu_2O was 0.2 mg cm^{-2} for both p-Cu_2O and WO_3/p-Cu_2O films, unless stated otherwise.

2.3. Characterization of films

The morphologies of the resulting films were examined with a scanning electron microscope (S3400, HITACHI, Japan). The crystalline structures of films were determined using an X-ray diffractometer (D/Max-RB, RIGAKU, Japan) with Cu Kα radiation ($\lambda = 0.15418$ nm). The diffractograms were obtained with a step width of 0.02° (2θ) and a scan rate of 8°/min.

2.4. Photocatalytic reactions

The obtained film (efficient area: $4\,cm^2$) was placed inside a cylinder quartz tube (filled with15 mL of 10 mg L^{-1} Orange II solution (pH = 5.7) or 15 mL of 0.4 mmol L^{-1} Cr(VI) solution (pH = 3.0), respectively.). A 300 W metal halide lamp was used as the stimulated natural light source, and the illumination density available at the film surface is about 14 mW cm^{-2} [24]. The concentrations of Orange II during the reaction period were determined spectrophotometrically by measuring the absorbance at 486 nm using a spectrophotometer (721E, Shanghai Spectra Instrument Co. Ltd, China). The concentrations of Cr(VI) were also measured using this spectrophotometer, but at 349 nm. Consequently, the degradation rate for Orange II and the reduction rate for Cr(VI) could be calculated according to the change in the absorbance. All the photocatalytic experiments were carried out at room temperature ($25 \pm 1\,^{\circ}C$) and without stirring.

Experiments on adsorption of Orange II and Cr(VI) by the different films were also carried out in a cylinder quartz tube, but under dark conditions. After 60-min adsorption, samples were withdrawn from the solutions and analyzed spectrophotometrically.

3. Results and discussion

3.1. Characterization of films

Fig. 1 shows the XRD patterns of some selected samples of WO_3, n-Cu_2O, p-Cu_2O, WO_3/n-Cu_2O and WO_3/p-Cu_2O films. For single WO_3 film (a), the diffraction pattern (Fig. 1(a)) corresponds to an orthorhombic $WO_3 \cdot H_2O$ phase (JCPDS 43-679), and the broad

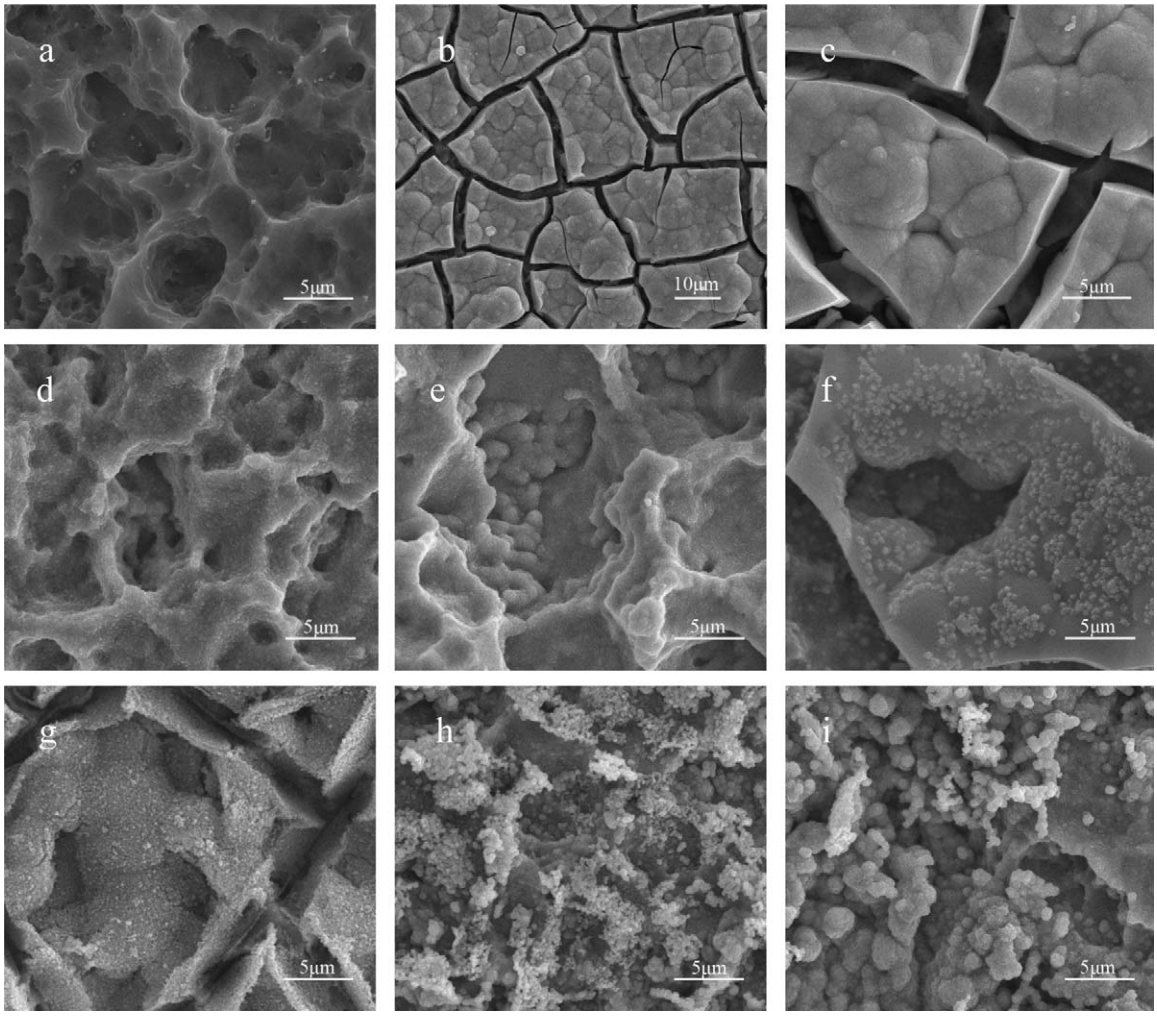

Fig. 2. SEM micrographs of Ti (a), WO_3 (b and c), n-Cu_2O (d), p-Cu_2O (e), WO_3/n-Cu_2O (f) and WO_3/p-Cu_2O films with different deposition amount of p-Cu_2O: 0.08 mg cm^{-2} (g), 0.4 mg cm^{-2} (h) and 0.8 mg cm^{-2} (i).

diffraction peak indicates the nanocrystalline nature of the film [28]. The mean crystallite size of WO_3 is 65 nm through the calculation according to the Scherrer equation.

As can be seen in Fig. 1(b)–(e), five characteristic peaks corresponding to cubic Cu_2O (JCPDS 34-1354) are observed for both single Cu_2O and WO_3/p-Cu_2O films.

The mean crystallite size of Cu_2O in n-Cu_2O, p-Cu_2O, WO_3/n-Cu_2O and WO_3/p-Cu_2O films is 44 nm, 47 nm, 56 nm and 37 nm, respectively. A major difference in XRD pattern between n-Cu_2O and p-Cu_2O films is that the diffraction peak for p-Cu_2O at 2θ (value of 36.43°) corresponding to the reflection from (1 1 1) crystal surfaces is more intensive (Fig. 1(b) and (c)). In addition, it is worthy noting that the WO_3 diffraction peak corresponding to WO_3 in Fig. 1(a) disappears in Fig. 1(d) and (e), indicating the crystal structure of WO_3 may be changed during deposition of n-Cu_2O or p-Cu_2O onto it.

Fig. 2 shows the SEM micrographs of some selected samples of WO_3, n-Cu_2O, p-Cu_2O, WO_3/n-Cu_2O and WO_3/p-Cu_2O with different deposition amount of p-Cu_2O. For comparison, SEM micrograph of Ti substrate is also given (Fig. 2(a)). A "cracked-mud" morphology is observed for single WO_3 (Fig. 2(b) and (c)), characterized by large patches-islands separated by cracks, which is similar to that in the reference [7]. It can be noticed that the particles of n-Cu_2O deposited on Ti substrate (Fig. 2(d)) are smaller in size than that of p-Cu_2O (Fig. 2(e)). The particle size of n-Cu_2O deposited on WO_3 (Fig. 2(f)) is not noticeably changed in comparison with its counterpart on Ti substrate. For WO_3/p-Cu_2O composite films, more and more surface of WO_3 is coated by p-Cu_2O with the increase in deposition amount of p-Cu_2O (Fig. 2(g)–(i)), and the corresponding particle size of p-Cu_2O becomes bigger and bigger.

3.2. Photocatalytic activity

Initially, direct photolysis of Orange II in the absence of catalysts and adsorption of Orange II onto the relevant catalysts under dark conditions were performed, respectively. The negligible change in Orange II concentrations was observed for direct photolysis experiment. The degradation rates for Orange II after 60 min over WO_3, n-Cu_2O and WO_3/n-Cu_2O films are given in Fig. 3. For comparison, the results from the adsorption experiments are also included. One can see that WO_3 film exhibits very low photocatalytic activity. This result is in agreement with the previous reports [8,9]. This was thought to mainly result from the low conduction band (CB) edge of WO_3 [13]. Although WO_3 possesses a strong oxidation power due to its low valence band (VB) edge (+3.1 V vs. NHE), the reduction potential of photogenerated electrons in the CB of WO_3 is 0.4 V vs. NHE, which is much more positive than the one-electron reduction potential of adsorbed oxygen ($O_2 + e^- + H^+ \rightarrow HOO^\bullet$, $E = -0.046$ V vs. NHE) [29,30]. Because the photogenerated electrons cannot be consumed by the locally adsorbed oxygen, they must recombine with the photogenerated holes in the VB of WO_3. This low photocatalytic

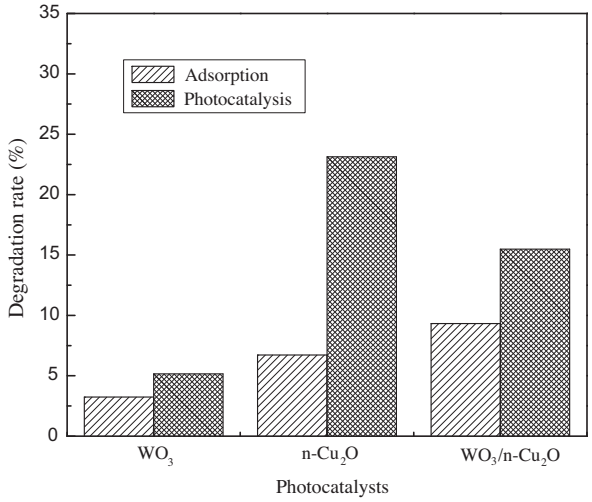

Fig. 3. Adsorption and photocatalytic degradation of Orange II for 60 min over WO_3, n-Cu_2O and WO_3/n-Cu_2O films.

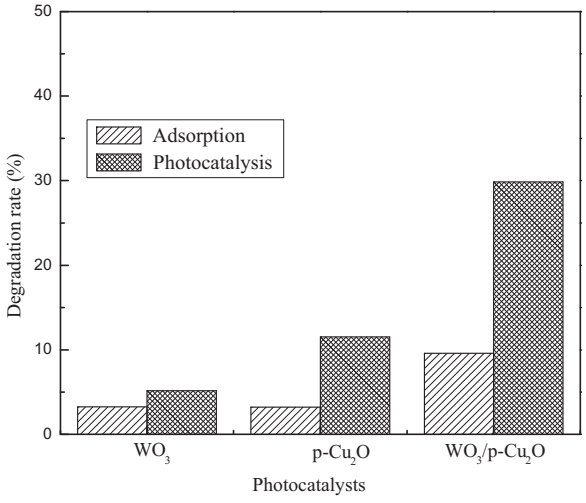

Fig. 5. Adsorption and photocatalytic degradation of Orange II for 60 min over WO_3, p-Cu_2O and WO_3/p-Cu_2O films.

activity of WO_3 film may result from the self-reduction process (Eq. (1)) by photogenerated electrons in WO_3 [31].

$$WO_3 + xe^- + xH^+ \rightarrow H_xW_{1-x}{}^{VI}W_x{}^{V}O_3 \quad (4)$$

In contrast, the results indicate that n-Cu_2O film exhibits higher photocatalytic activity than that of WO_3. In fact, it has been reported that Cu_2O is effective as a photocatalyst for photodegradation of methyl orange or Orange II under visible light illumination [32–34].

It is worthy noting that WO_3/n-Cu_2O film shows higher photocatalytic activity in comparison with single WO_3 film, but lower in comparison with single n-Cu_2O film, although the adsorption capacity of WO_3/n-Cu_2O is enhanced. The similar results were also obtained for ZnO/Cu_2O and TiO_2/Cu_2O composite photocatalysts by others [33,34]. The suppression of photocatalytic activity for n-Cu_2O when it is combined with WO_3 can be interpreted using a schematic diagram of energy band structure of WO_3/Cu_2O film shown in Fig. 4.

Under simulated natural light illumination, the electrons in VB of Cu_2O and WO_3 are excited to their corresponding CB according to processes (1) and (3) shown in Fig. 4, respectively. The CB edge of Cu_2O (−0.28 V vs. NHE) is higher than that of WO_3 (+0.4 V vs. NHE); the VB edges of Cu_2O and WO_3 are situated at +1.92 and +3.1 V vs. NHE, respectively [29,30,35]. From thermodynamic view points, the photogenerated electrons transfer from CB of Cu_2O to that of WO_3 (process (2)), while the photogenerated holes immigrate in the opposite direction from VB of WO_3 to that of Cu_2O (process (4)). Because it is impossible for the photogenerated electrons in the CB of WO_3 to be consumed by the adsorbed oxygen through one-electron reduction, such a charge transfer weaken the stronger reduction power of photogenerated electrons in the CB of Cu_2O. As a result, WO_3/n-Cu_2O composite film shows photocatalytic activity lower than single n-Cu_2O film. This mechanism can also be used to explain the similar results obtained by others for ZnO/Cu_2O and TiO_2/Cu_2O composite photocatalysts [33,34].

For WO_3/p-Cu_2O composite film, the results are quite different from WO_3/n-Cu_2O (see Fig. 5). Contrary to the case of n-Cu_2O, single p-Cu_2O film exhibits low photocatalytic activity. More importantly, WO_3/p-Cu_2O composite film exhibits the highest activity among the five films tested. Although the increase in adsorption capacity of WO_3/p-Cu_2O favors its photocatalytic activity, it is more likely that in case of WO_3/p-Cu_2O composite film exists a different mechanism for photogenerated charges transfer between the two semiconductor materials, which can be explained based on the model of the p–n photochemical diode shown in Fig. 6 [16,17], rather than the charge separation model (shown in Fig. 4). In this p–n heterojunction, the majority electron in WO_3 and the majority hole in p-Cu_2O would combine by transfer through the interface between the two semiconductors (process (3)), while the recombination

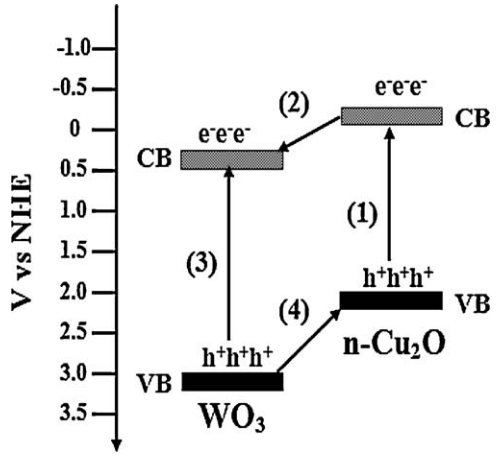

Fig. 4. Schematic diagram for charge-transfer process in WO_3/n-Cu_2O composite film.

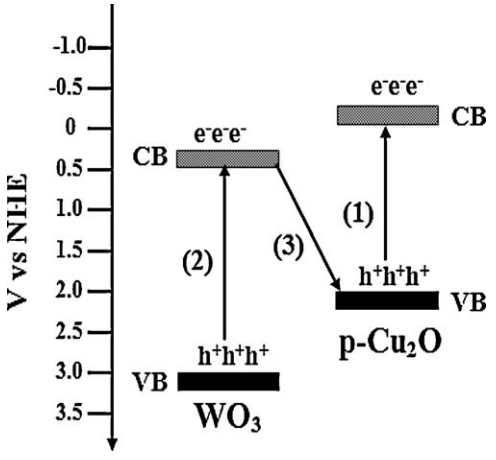

Fig. 6. Schematic diagram for charge-transfer process in WO_3/p-Cu_2O composite film.

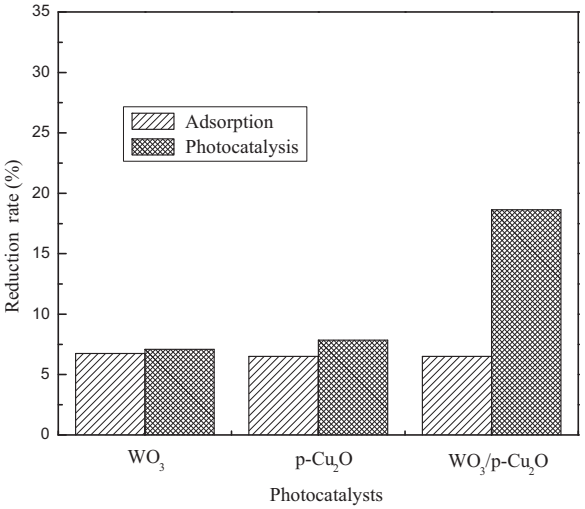

Fig. 7. Adsorption and photocatalytic reduction of Cr(VI) for 60 min over WO_3, p-Cu_2O and WO_3/p-Cu_2O films.

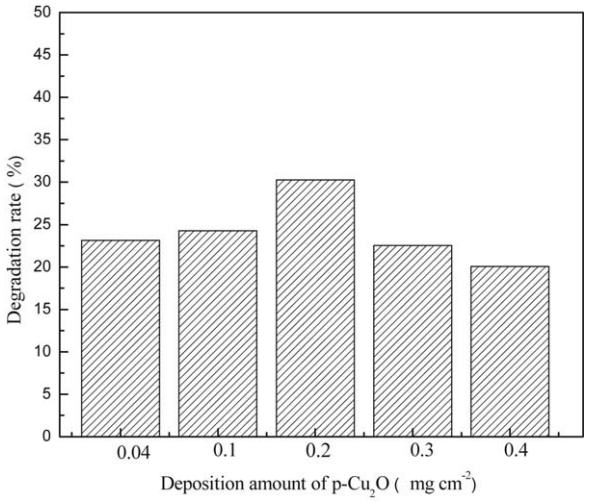

Fig. 8. Effect of deposition amount of p-Cu_2O in WO_3/p-Cu_2O composite films on degradation rate for Orange II for 60 min.

of photogenerated charges in the respective semiconductors would be suppressed. Consequently, the photogenerated electrons with strong reduction power in the CB of Cu_2O and the photogenerated holes with strong oxidation power in the VB of WO_3 are kept. In such a case, two photons must be absorbed to generate one net electron–hole pair for redox reactions at the photocatalyst surface. The photocatalytic oxidation pathway for Orange II over WO_3/p-Cu_2O composite film can be simply expressed as follows:

$$WO_3/Cu_2O + h\nu \rightarrow WO_3(e^- + h^+)/Cu_2O(e^- + h^+) \quad (5)$$

$$WO_3(e^- + h^+)/Cu_2O(e^- + h^+) \rightarrow WO_3(h^+)/Cu_2O(e^-) \quad (6)$$

$$O_2 + e^- + H^+ \rightarrow HOO^{\bullet} \quad (7)$$

$$HOO^{\bullet} + \text{Orange II} \rightarrow \text{products} \quad (8)$$

$$h^+ + \text{Orange II} \rightarrow \text{products} \quad (9)$$

In order to further illustrate the mechanism for WO_3/p-Cu_2O composite film, the photocatalytic reduction of Cr(VI) over WO_3/p-Cu_2O, WO_3 and p-Cu_2O film in the absence of other reducing agents (hole scavengers) were investigated, respectively. For comparison, adsorption experiments of those samples under dark conditions were also performed. The total time of both reaction and adsorption was 60 min. The obtained results are given in Fig. 7. It is obvious that the adsorption amount of Cr(VI) onto the three photocatalysts is almost the same. Because the VB edge of Cu_2O is only +1.92 V vs. NHE and the oxidation of water by holes is kinetically sluggish, which leads to a fast recombination rate for electron-hole pairs photogenerated, p-Cu_2O shows low photocatalytic activity towards reduction of Cr(VI). Considering the fact that reduction potential of photogenerated electrons in the CB of WO_3 (+0.4 V vs. NHE) is more negative than that of Cr(VI) ($Cr_2O_7^{2-} + 14H^+ + 6e^- \rightarrow 2Cr^{3+} + 7H_2O$, E = 1.33 V vs. NHE) [36], and its VB edge (+3.1 V vs. NHE) is positive enough to oxidize H_2O to O_2 ($2H_2O\text{-}4e^- \rightarrow O_2 + 4H^+$, E = +1.23 V vs. NHE) [29], WO_3 should have acted as an efficient photocatalyst for reduction of Cr(VI) even without other reducing agents. The low photocatalytic activity of WO_3 may also be attributed to the easy recombination of charge carriers photogenerated [10]. However, as mentioned above, WO_3/p-Cu_2O heterojunction prevents the charge carriers from recombination within respective semiconductors and keep the photogenerated electrons with strong reduction power and the photogenerated holes with strong oxidation power. As a result, WO_3/p-Cu_2O composite film exhibits high photocatalytic activity towards reduction of Cr(VI).

In a composite semiconductor with bilayer structure, the amount (or the thickness) of coating component (i.e. the upper layer of composite film) plays an important role in its photocatalytic activity [37]. Therefore, the experiments on photocatalytic degradation of Orange II for 60 min over WO_3/p-Cu_2O composite films with different deposition amount of p-Cu_2O were carried out. The results are shown in Fig. 8. When the deposition amount of p-Cu_2O is less than 0.2 mg cm^{-2}, the photocatalytic activity of WO_3/p-Cu_2O composite films increases with increasing the deposition amount of p-Cu_2O. After that, the photocatalytic activitiy of the composite films starts to decrease. This indicates that an appropriate deposition amount of p-Cu_2O exists in WO_3/p-Cu_2O composite films in respect of photocatalytic activitiy. In the case of little deposition amount of p-Cu_2O, the contact area between the two semiconductors is smaller, which results in production of less charge carriers taking part in the redox reactions. On the other hand, when the deposition amount of p-Cu_2O is too large, the efficient number of photons reaching the composite semiconductor interface is reduced due to a high absorption coefficient of Cu_2O [21]. Furthermore, the oxidation of Orange II by holes at WO_3 surface is also seriously hindered under these circumstances.

Apart from the high photocatalytic activity, the stability or recycling performance of a photocatalyst is an important factor for its practical application [2]. Three cycling runs in the photocatalytic oxidation of Orange II over WO_3/p-Cu_2O composite film under simulated natural light illumination were carried out. The reaction time was limited to 60 min for each run. The results from cycling runs are shown in Fig. 9. The photocatalytic activity does not exhibit a significant loss after three recycles for the photocatalytic oxidation of Orange II. This indicates that the WO_3/p-Cu_2O composite film has a relatively high stability during the photocatalytic oxidation of Orange II. This result is possibly related to the charge transfer mechanism between the interfaces of WO_3/p-Cu_2O shown in Fig. 4. In view of the VB potential of Cu_2O (+1.92 vs. NHE) and that of Cu(II)/Cu(I) redox couple (0.16 V vs. NHE) [38], the oxidation of Cu_2O by holes in its VB (Eq. (7)) may take place.

$$Cu_2O + 2OH^- + 2h^+ \rightarrow 2CuO + H_2O \quad (10)$$

This is so-called photocorrosion of Cu_2O. In a previous work by others [39], it has been found that Cu_2O nanoparticles are very easy to be photocorroded during photocatalytic reaction, resulting in a deactivation of the photocatalyst. However, for WO_3/p-Cu_2O, the combination of the electrons in CB of WO_3 with the holes in VB of p-Cu_2O prevents p-Cu_2O from photocorrosion at least to some

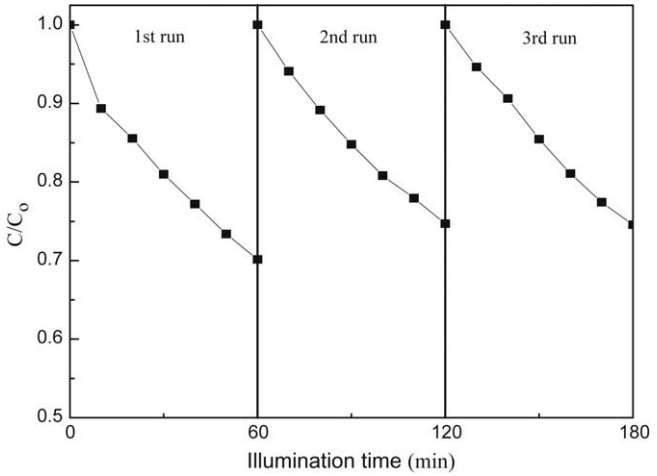

Fig. 9. Cycling runs in photocatalytic degradation of Orange II over WO_3/p-Cu_2O composite film. C_0 and C represent the initial concentration of Orange II and that at given reaction time, respectively.

extent. The lower photocatalytic activity of WO_3/n-Cu_2O than n-Cu_2O may also be partly ascribed to the easier photocorrosion of n-Cu_2O in the composite film due to the accumulation of holes in it. The detailed influence of those heterojunctions on photocorrosion of n-Cu_2O and p-Cu_2O semiconductors is under investigation in our laboratory.

4. Conclusions

The following conclusions can be withdrawn from the results in the present work: WO_3/n-Cu_2O and WO_3/p-Cu_2O composite films can be fabricated on a conducting substrate with a consecutive cathodic electrodeposition route. Cu_2O films obtained from different electrolyte solutions exhibit different photocatalytic activity. The enhancement of photocatalytic activity compared to single Cu_2O is achieved only in the case of combination of p-Cu_2O with WO_3. Furthermore, the photocatalytic activity of WO_3/p-Cu_2O composite film is better than WO_3/n-Cu_2O. For WO_3/p-Cu_2O composite film, the deposition amount of p-Cu_2O plays an important role in determining its photocatalytic activity, and an optimal value exists in a given range. The difference in photocatalytic activity between WO_3/n-Cu_2O and WO_3/p-Cu_2O composite films implies that there are different mechanisms for transfer of photogenerated charge carriers in the two heterojunctions. WO_3/p-Cu_2O composite film may be a promising photocatalyst due to its photocatalytic activity and stability.

References

[1] A. Fujishima, T.N. Rao, D.A. Tryk, Titanium dioxide photocatalysis, J. Photochem. Photobiol. C 1 (2000) 1–21.
[2] J. Yu, L. Qi, Template-free fabrication of hierarchically flower-like tungsten trioxide assemblies with enhanced visible-light-driven photocatalytic activity, J. Hazard. Mater. 169 (2009) 221–227.
[3] N.M. Mahmoodi, M. Arami, N.Y. Limaee, N.S. Tabrizi, Decolorization and aromatic ring degradation kinetics of direct red 80 by UV oxidation in the presence of hydrogen peroxide utilizing TiO_2 as a photocatalyst, Chem. Eng. J. 112 (2005) 191–196.
[4] X. Xu, H. Li, J. Gu, Simultaneous decontamination of hexavalent chromium and methyl *tert*-butyl ether by UV/TiO_2 process, Chemosphere 63 (2006) 254–260.
[5] A. Watcharenwong, W. Chanmanee, N.R. de Tacconi, C.R. Chenthamarakshan, P. Kajitvichyanukul, K. Rajeshwar, Anodic growth of nanoporous WO_3 films: morphology, photoelectrochemical response and photocatalytic activity for methylene blue and hexavalent chrome conversion, J. Electroanal. Chem. 612 (2008) 112–120.
[6] M. Yagi, S. Maruyama, K. Sone, K. Nagai, T. Norimatsu, Preparation and photoelectrocatalytic activity of a nano-structured WO_3 platelet film, J. Solid State Chem. 181 (2008) 175–182.
[7] J. Georgieva, S. Armyanov, E. Valova, I. Poulios, S. Sotiropoulos, Enhanced photocatalytic activity of electrosynthesised tungsten trioxide–titanium dioxide bi-layer coatings under ultraviolet and visible light illumination, Electrochem. Commun. 9 (2007) 365–370.
[8] C. Lin, C. Wu, Z. Onn, Degradation of 4-chlorophenol in TiO_2, WO_3, SnO_2, TiO_2/WO_3 and TiO_2/SnO_2 systems, J. Hazard. Mater. 154 (2008) 1033–1039.
[9] S. Sakthivel, S.U. Geissen, D.W. Bahnemann, V. Murugesan, A. Vogelpohl, Enhancement of photocatalytic activity by semiconductor heterojunctions: α-Fe_2O_3, WO_3 and CdS deposited on ZnO, J. Photochem. Photobiol. A 148 (2002) 283–293.
[10] H. Kim, Y. Tak, K. Senthil, J. Joo, S. Jeon, K. Yong, Novel heterostructure of CdS nanoparticle/WO_3 nanowhisker: synthesis and photocatalytic properties, J. Vac. Sci. Technol. B 27 (2009) 2182–2186.
[11] D. Ke, H. Liu, T. Peng, X. Liu, K. Dai, Preparation and photocatalytic activity of WO_3/TiO_2 nanocomposite particles, Mater. Lett. 62 (2008) 447–450.
[12] Y.T. Kwon, K.Y. Song, W.I. Lee, G.J. Choi, Y.R. Do, Photocatalytic behavior of WO_3-loaded TiO_2 in an oxidation reaction, J. Catal. 191 (2000) 192–199.
[13] Z. Liu, Z.G. Zhao, M. Miyauchi, Efficient visible light active $CaFe_2O_4$/WO_3 based composite photocatalysts: effect of interfacial modification, J. Phys. Chem. C 113 (2009) 17132–17137.
[14] W. Luo, T. Yu, Y. Wang, Z. Li, J. Ye, Z. Zou, Enhanced photocurrent–voltage characteristics of WO_3/Fe_2O_3 nano-electrodes, J. Phys. D 40 (2007) 1091–1096.
[15] P. Chatchai, Y. Murakami, S. Kishioka, A.Y. Nosaka, Y. Nosaka, Efficient photocatalytic activity of water oxidation over WO_3/$BiVO_4$ composite under visible light irradiation, Electrochim. Acta 54 (2009) 1147–1152.
[16] T. Arai, M. Yanagida, Y. Konishi, Y. Iwasaki, H. Sugihara, K. Sayama, Efficient complete oxidation of acetaldehyde into CO_2 over $CuBi_2O_4$/WO_3 composite photocatalyst under visible and UV light irradiation, J. Phys. Chem. C 111 (2007) 7574–7577.
[17] C. Hu, J. Nian, H. Teng, Electrodeposited p-type Cu_2O as photocatalyst for H_2 evolution from water reduction in the presence of WO_3, Sol. Energy Mater. Sol. Cells 92 (2008) 1071–1076.
[18] D. Lincot, Electrodeposition of semiconductors, Thin Solid Films 487 (2005) 40–48.
[19] J.S. Wellings, N.B. Chaure, S.N. Heavens, I.M. Dharmadasa, Growth and characterisation of electrodeposited ZnO thin films, Thin Solid Films 516 (2008) 3893–3898.
[20] J. Nishino, S. Chatani, Y. Uotani, Y. Nosaka, Electrodeposition method for controlled formation of CdS films from aqueous solutions, J. Electroanal. Chem. 473 (1999) 217–222.
[21] K. Han, M. Tao, Electrochemically deposited p–n homojunction cuprous oxide solar cells, Sol. Energy Mater. Sol. Cells 93 (2009) 153–157.
[22] W. Siripala, L.D.R.D. Perera, K.T.L. de Silva, J.K.D.S. Jayanetti, I.M. Dharmadasa, Study of annealing effects of cuprous oxide grown by electrodeposition technique, Sol. Energy Mater. Sol. Cells 44 (1996) 251–260.
[23] S. Wei, Z. Shao, X. Lu, Y. Liu, L. Cao, Y. He, Photocatalytic degradation of methyl orange over ITO/CdS/ZnO interface composite films, J. Environ. Soc. 21 (2009) 991–996.
[24] S. Wei, Y. Chen, Y. Ma, Z. Shao, Fabrication of CuO/ZnO composite films with cathodic co-electrodeposition and their photocatalytic performance, J. Mol. Catal. A 331 (2010) 112–116.
[25] E.A. Meulenkamp, Mechanism of WO_3 electrodeposition from peroxytungstate solution, J. Electrochem. Soc. 144 (1997) 1664–1671.
[26] R.P. Wijesundera, M. Hidaka, K. Koga, M. Sakai, W. Siripala, Growth and characterisation of potentiostatically electrodeposited Cu_2O and Cu thin films, Thin Solid Films 500 (2006) 241–246.
[27] F. Hu, K.C. Chan, T.M. Yue, Morphology and growth of electrodeposited cuprous oxide under different values of direct current density, Thin Solid Films 518 (2009) 120–125.
[28] H. Habazaki, Y. Hayashi, H. Konno, Characterization of electrodeposited WO_3 films and its application to electrochemical wastewater treatment, Electrochim. Acta 47 (2002) 4181–4188.
[29] T. Torimoto, N. Nakamura, S. Ikeda, B. Ohtani, Discrimination of the active crystalline phases in anatase–rutile mixed titanium(IV) oxide photocatalysts through action spectrum analyses, Phys. Chem. Chem. Phys. 4 (2002) 5910–5914.
[30] M. Miyauchi, Photocatalysis and photoinduced hydrophilicity of WO_3 thin films with underlying Pt nanoparticles, Phys. Chem. Chem. Phys. 10 (2008) 6258–6265.
[31] C. Bechinger, G. Oefinger, S. Herminghaus, P. Leiderer, On the fundamental role of oxygen for the photochromic effect of tungsten trioxide, J. Appl. Phys. 74 (1993) 4527–4533.
[32] X. Zhang, J. Song, J. Jiao, X. Mei, Preparation and photocatalytic activity of cuprous oxides, Solid State Sci. 12 (2010) 1215–1219.
[33] C. Xu, L. Cao, G. Su, W. Liu, H. Liu, Y. Yu, X. Qu, Preparation of ZnO/Cu_2O compound photocatalyst and application in treating organic dyes, J. Hazard. Mater. 176 (2010) 807–813.
[34] L. Huang, F. Peng, H. Wang, H. Yu, Z. Li, Preparation and characterization of Cu_2O/TiO_2 nano–nano heterostructure photocatalysts, Catal. Commun. 10 (2009) 1839–1843.
[35] Y. Xu, M.A.A. Schoonen, The absolute energy positions of conduction and valence bands of selected semiconducting minerals, Am. Mineral. 85 (2000) 543–556.
[36] M.I. Litter, Heterogeneous photocatalysis transition metal ions in photocatalytic systems, Appl. Catal. B 23 (1999) 89–114.

[37] J. Shang, W. Yao, Y. Zhu, N. Wu, Structure and photocatalytic performances of glass/SnO_2/TiO_2 interface composite film, Appl. Catal. A 257 (2004) 25–32.
[38] H. Irie, S. Miura, K. Kamiya, K. Hashimoto, Efficient visible light-sensitive photocatalysts: grafting Cu (II) ions onto TiO_2 and WO_3 photocatalysts, Chem. Phys. Lett. 457 (2008) 202–205.
[39] L. Huang, F. Peng, H. Yu, H. Wang, Preparation of cuprous oxides with different sizes and their behaviors of adsorption, visible-light driven photocatalysis and photocorrosion, Solid State Sci. 11 (2009) 129–138.